On the distribution and productivity of mountain grasslands in the Gran Paradiso National Park, NW Italy: A remote sensing approach

Gianluca Filippa, Edoardo Cremonese, Marta Galvagno, Arthur Bayle, Philippe Choler, Mauro Bassignana, Anaïs Piccot, Laura Poggio, Ludovica Oddi, Simon Gascoin, et al.

International Journal of Applied Earth Observations and Geoinformation 108 (2022) 102718

Contents lists available at ScienceDirect

International Journal of Applied Earth Observations and Geoinformation

journal homepage: www.elsevier.com/locate/jag

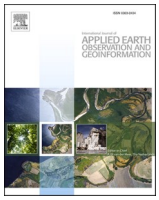

On the distribution and productivity of mountain grasslands in the Gran Paradiso National Park, NW Italy: A remote sensing approach

Gianluca Filippa [a,*], Edoardo Cremonese [a], Marta Galvagno [a], Arthur Bayle [b], Philippe Choler [b], Mauro Bassignana [c], Anaïs Piccot [c], Laura Poggio [d], Ludovica Oddi [e], Simon Gascoin [f], Sergi Costafreda-Aumedes [g,h], Giovanni Argenti [h], Camilla Dibari [h]

[a] Environmental Protection Agency of Aosta Valley - Climate Change Unit, Saint-Christophe, Italy
[b] Univ. Grenoble Alpes, Univ. Savoie Mont Blanc, CNRS, LECA, Grenoble, France
[c] Institut Agricole Régional, Aosta, Italy
[d] Ufficio Conservazione botanico-forestale, Servizio Ricerca scientifica e Biodiversitá, Parco nazionale Gran Paradiso, Torino, Italy
[e] Department of Life Sciences and Systems Biology, University of Torino, Torino, Italy
[f] CESBIO, Université de Toulouse, CNES/CNRS/IRD/INRAE/UPS, Toulouse, France
[g] Consiglio Nazionale delle Ricerche-Istituto per la Bioeconomia (CNR-IBE), Florence, Italy
[h] Department of Agriculture, Food, Environment and Forestry (DAGRI), University of Florence, Florence, Italy

ARTICLE INFO

Keywords:
NDVI
Pasture categories
Pastoral resources
Random forest
Sentinel 2

ABSTRACT

Mountain grazing lands are key constituents of the natural, economical and cultural heritage, but at the same time sensitive to climate and land use change, hence requiring urgent adaptation and management strategies. These must be based on a better understanding of the distribution of mountain pastoral resources across space and time.

In this study we model the distribution and the productivity of grassland surfaces in a topographically complex protected area (Gran Paradiso National Park, 710 km^2) in north-western Italian Alps. The objective of our work was threefold: a) modelling the distribution of mountain grasslands across the entire park at a 20-meters spatial resolution, b) classify pastoral surfaces according to productivity classes, and c) according to thirteen pastoral categories. We used a random forest approach to combine a massive terrain vegetation survey as ground truth, with remote-sensing-derived, climatic and topographic layers as predictors.

Grassland presence/absence was classified with high accuracy (up to 88%) and, compared to the standard Copernicus European Grassland Product, revealed the presence of extensive high altitude grassland areas potentially available for wild herbivores. Grassland productivity was modelled with remarkably high accuracy both according to three broad productivity classes (90% accuracy) and to a more detailed classification into thirteen pastoral categories (83% accuracy). Productivity estimates agree well with satellite-derived leaf area index maps and with area-averaged NDVI seasonal patterns.

We conclude that combining tailored field campaigns and high-resolution remote sensing allows for robust prediction of grassland distribution and productivity even in complex terrains. This information can contribute to improve the management of pastoral resources and promote effective adaptation strategies.

1. Introduction

Covering 26% of the global land area, and 70% of the agricultural surfaces worldwide (Ramankutty et al., 2008), grasslands stand as one of the most prevalent and widespread land cover types. They are important regulators of carbon and water cycles (Conant et al., 2010), a biodiversity reservoir (Körner, 2004) and food for livestock (Pornaro et al., 2019). Nevertheless, they are threatened by several factors including overgrazing, the abandonment of agricultural practices (Garbarino et al., 2020), and climate change, which, all together, have reduced grassland areas globally (Chang et al., 2021; Urbina et al., 2020; Ponzetta et al., 2010).

In the Alps, the vast majority of mountain grasslands are permanent grasslands that play important economical and cultural roles, being a

* Corresponding author.
E-mail address: g.filippa@arpa.vda.it (G. Filippa).

https://doi.org/10.1016/j.jag.2022.102718
Received 8 November 2021; Received in revised form 14 January 2022; Accepted 9 February 2022
Available online 18 February 2022

key constituent of vertical transhumance systems. Because climate and land use change in the last decades are threatening these ecosystems (Herzog et al., 2018; Hinojosa et al., 2019; Dibari et al., 2021, 2020), several projects were proposed to assess vulnerability, and subsequently facilitate the implementation of adaptation strategies for pastoral management (Pittarello et al., 2019). For global change adaptation and mitigation to take place, detailed quantification of alpine pastoral resources (mapping) is pivotal (e.g., Schwieder et al., 2022). It is required in order to understand the actual status of mountain grassland ecosystems and their current trajectories in terms of gain, conservation or loss (Monteiro et al., 2021). For example, these trajectories were found to vary considerably across space and time in Tyrol, mediated by socio-economical and bio-physical factors (Hinojosa et al., 2019). Moreover, several studies documented high responsiveness of climate-warming-induced greening in scarcely vegetated, high altitude areas (e.g., Choler et al., 2021), but a quantitative assessment of how much these changing environments contribute to the pastoral resources remains to be conducted. Mapping of mountain grasslands is nevertheless hampered by complex topography, remoteness and small scale heterogeneity that characterize mountain pastures (Orlandi et al., 2016). This makes it difficult to map pasture types and productivity exclusively on the basis of field surveys (Dibari et al., 2016). Mapping supported by earth observation data may be of help, but before the recent Sentinel era coarse spatial resolution and long revisiting time strongly limited its use in mountain areas. The Copernicus Land Monitoring Service recently released a grassland product, consisting of a presence/absence map at 10-m spatial resolution for the whole Europe and for the year 2018 (Copernicus, 2018b). This layer was obtained by combining Sentinel S-2 L2A-data, S-2 LC1-data and S-1 data. A reliability assessment of this layer in complex terrain at the scale of small catchments is however lacking. Nation-wide mapping of grasslands was recently realized for Germany (Griffiths et al., 2020), and for Switzerland (Pazúr et al., 2021). In particular, Pazúr et al., 2021 suggested better performance for classification models trained and applied at regional-to-national scale, rather than larger scale, due to better parametrization of models.

Remote sensing data streams are commonly coupled with machine learning algorithms for land cover and land use classification (e.g. Abdi, 2020), crop mapping, and, recently, the detection of mowing and other agricultural practices (Kolecka et al., 2018; Reinermann et al., 2020). Pixel-based supervised classification exploiting Sentinel-2 data has been object of a great number of agro-ecological studies after Sentinel launch in 2015 (Phiri et al., 2020; Punalekar et al., 2021). Generally, machine learning methods are applied to multispectral satellite data or derived vegetation indexes to directly model biomass from in situ measurements and vegetation indexes (see Reinermann et al., 2020, and reference therein). In this context, it has been suggested that modelling of mountain pasture biomass could be strongly improved by coupling remotely sensed vegetation indexes and vegetation maps (Magiera et al., 2017). The use of supervised classification for the determination of subtle differences of productivity in mountain grasslands, at a scale as fine as the distinction of pastoral categories is still a rather unexplored field of application (Crabbe et al., 2020).

In the context of the EU LIFE project "Pastures vulnerability and adaptation strategies to climate change impacts in the Alps" (PASTORALP, Argenti et al., 2018), a joint effort was made to find a common, transnational classification key for the most important pasture types in two national parks on the French (Ecrins National Park) and on the Italian side (Gran Paradiso National Park, GPNP) of the western Alps. The resulting classification method identified thirteen grassland categories (Bassignana et al., 2021) and was used in GPNP to map pastoral resources in the most important pastoral districts.

In this work, we combined the results of the PASTORALP surveys with remote sensing data through a machine learning approach. The main objective of our work was threefold: a) modelling the distribution of mountain grassland areas across the whole Gran Paradiso National Park at a 20-m spatial resolution; and b) the classification of pastoral surfaces according to a broad distinction into three productivity classes, and c) the classification of grasslands according to the above-mentioned thirteen pastoral categories.

2. Materials and methods

2.1. Study area

This study was conducted in the Gran Paradiso National Park, located in the western Italian Alps. Covering a surface of >710 km^2 and an elevation range of 800–4061 m asl, it is the oldest Italian protected area. Grasslands constitute approximately 54% of the park, whereas the remaining surface is covered by forests or shrublands (18%), bare surfaces (20%), and permanent snow and ice (7%; Buchhorn et al., 2019). About half of the grassland areas are considered as pastoral surfaces (Canedoli et al., 2020), and many of these are located in areas under special protection. Consequently, only about one third of them are currently subjected to pastoral activities, which consist mainly of cattle and goat grazing during the summer months (Canedoli et al., 2020).

2.2. Ground truth

In order to model the presence or absence of grasslands (objective 1) we used a pre-existent land cover map. In a previous work (Filippa et al., 2019) vegetation types were mapped by photo-interpretation and aggregated in 3 land covers: 1) grasslands, 2) forests, 3) ice/snow/water, bare rocks. This map (20 m spatial resolution) is hereafter referred to as Carta della Natura (CDN).

In order to model the productivity and types of grasslands (objective 2 and 3) we exploited the above mentioned PASTORALP surveys. Pastures were mapped and classified in the field following the three most important approaches adopted in the western Italian and French Alps (Bornard et al., 2006; Cavallero et al., 2007; Jouglet, 1999). The three methods were combined in order to obtain a common classification scheme that could be deployed in the framework of the LIFE PASTORALP project. Details on this classification harmonization and mapping are reported in a dedicated publication (Bassignana et al., 2021). It is important to highlight the following features:

1. A total surface of ~69 km^2 was mapped (i.e., 17% of the grassland surfaces of the park), corresponding to the main pastoral districts (Fig. 1). These were digitized and stored as polygonal vectors.
2. Thirteen categories were established based on the physiognomy of the pasture, the topography (i.e., altitude, aspect and slope), the productivity and the presence of dominant species (Table 1). In particular, productivity ranges and potential stocking rates were assigned to the thirteen categories based on a historical database of dry biomass production (Bornard et al., 2006; Jouglet, 1999), thus establishing a direct linkage between pastoral categories and productivity (Table 1). Additionally, the thirteen categories were further grouped into three broader classes of productivity, high (HP), medium (MP) and low productive (LP) pastures (Table 2).
3. A special effort was made to determine the net grazing area of pastoral surfaces, by identifying the portion of non-grazeable areas at the scale of the individual polygons. Features that reduce the grazing potential of grasslands include shrubs, single or groups of trees, bare rocks, debris, buildings or water bodies. From the remote sensing perspective, these features can contribute to increase noise in signal retrieval. Accordingly, surfaces were classified as fully grazeable (FG) when 95–100% of the surface was mapped as pasture, half grazeable (HG) when the net grazeable surface ranged between 50% and 95% and poorly grazeable (PG) below 50% (Table 2).

A representative small-scale map of PASTORALP survey is reported in the supplementary material (figure SF1).

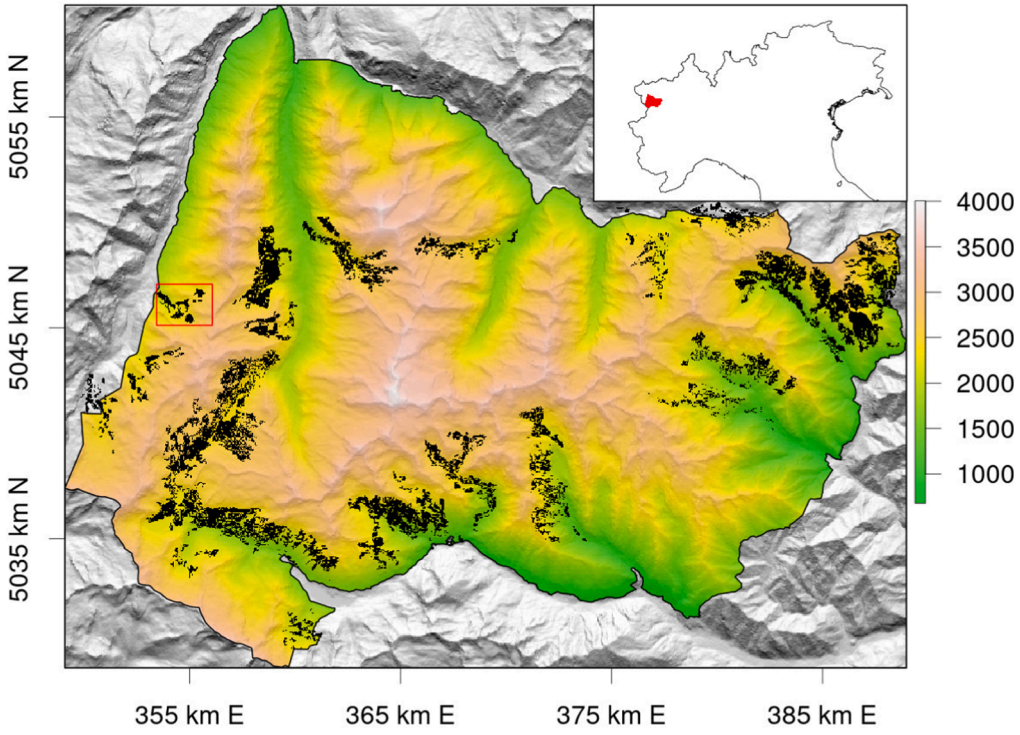

Fig. 1. The extent of pastoral areas in the Gran Paradiso National Park that were used as ground truth in this study (black polygons). Color gradient represents digital elevation model. Inset: northern Italy with the location of the Park in red. The red rectangle on the western part of the park is the extent of the high resolution image in the Supplementary material (figure SF1).

2.3. Remote sensing and climatic data

In this section, we describe the gridded datasets that were used to predict grasslands distribution and productivity. All the layers were re-projected, when needed, to WGS 84 32 N (EPSG:32632).

2.3.1. Vegetation indices

We downloaded all the available Sentinel-2 multispectral images (tile 32TLR) for the period 2017 to 2019, at the 2A level, atmospherically and topographically corrected with the sen2cor processor. The images were filtered on a per-pixel basis with the scene classification (SCL) map, retaining only top quality, cloud- and shadow-free pixels. NDVI was calculated from 20-m-resolution bands for each available date and a maximum yearly composite was calculated for each separate year and then averaged over the three-year period.

In addition to the maximum composite NDVI, we also calculated pixel-wise integrals of NDVI seasonl trajectories and averaged the resulting maps over the three-year period. Using the same Sentinel images, we computed the Normalized Anthocyanin Reflectance Index (NARI, Bayle et al., 2019). Values of this index in autumn are particularly effective in the discrimination between grasslands and shrubs such as *Ericaceae* (Bayle et al., 2019).

The Copernicus tree cover density layer for 2018 (20-m spatial resolution, Copernicus, 2018c) was used to define dense and sparse forest areas. The Copernicus Grassland layer for 2018 at 10 m spatial resolution (Copernicus, 2018b) was used as a comparative layer for the grassland absence/presence map. Finally, a maximum composite Leaf Area Index was computed from Sentinel-derived S2 multi-temporal Leaf Area Index images obtained with the biophysical processor available in the Sentinel-2 toolbox (Xie et al., 2019; Weiss and Baret, 2016). Although this layer cannot be considered as fully independent, being itself derived from Sentinel-2 data stream, it was used as a comparative layer for the grassland productivity map.

2.3.2. Climate and topography

We used first snow free day maps (FSFD) produced by Theia Data and Services centre as part of Sentinel L3B-snow product (Gascoin et al., 2019). The FSFD (also named SMD, i.e., snow melt-out date) corresponds to the last day of the longest snow-covered period in the hydrological year (starting on 1 September). The 20 m resolution maps for the period 2017–2019 were averaged to obtain a mean FSFD map. This was included as a predictor itself but also used to compute a growing-degree-days map (GDD) where temperatures >0 °C were cumulated from FSFD until day of the year 270 (September, 26*th*, a fall date when temperature is expected to no longer affect plant development). GDD computation is often restricted to the growing season (e.g., the end of August; Choler, 2018). Here we decided to extend the time interval to doy 270 because several pastoral districts are used until mid September. Daily temperature maps at 100-m spatial resolution, used to compute GDD, were available for the period 2000-today (Silvestro et al., 2013, 2015).

We used a digital elevation model from the Shuttle Radar Topography Mission (native spatial resolution ~30 m, Farr et al., 2007) to calculate the diurnal anisotropic heating index (DAH; Böhner and Antonic, 2009). DAH represents an approximation of the radiative heating potential of a given pixel based on its slope and aspect and therefore can be used as a proxy of how favourable a location is to plant growth in terms of temperature.

2.4. Data analysis

2.4.1. Dynamic time warping analysis

Multitemporal NDVI and NARI stacks were used to perform a dynamic time warping analysis (DTW, Giorgino, 2009). DTW is a suite of algorithms that allows computing distances between time series. We used an implementation of the algorithms specific for satellite data available in the R package `dtwSat` (Maus et al., 2019). We first

Table 1
Characteristics of pastures used as ground truth in this study. Total pasture surface amounts to ~69 km^2. Pasture categories are named according to the altitudinal band they belong to (A: alpine, S: subalpine, SA: both subalpine and alpine), and with increasing Roman numerals corresponding to decreasing potential stocking rate. LSU: livestock units, RSE: relative standard error (%).

Pasture category	Description	Mean Productivity [g m^{-2}] (RSE, %)	Potential stocking rate [LSU d/ha]	Surface [km^2] (%)	Productivity class
S-I	Vegetation in flatlands and low slopes of the subalpine level with rich soil. Very tall (over 50 cm) and very dense vegetation dominated by broad-leaved grasses	325 (25%)	80–130	2.9 (4.2%)	high prod.
S-II	Vegetation in flatlands and low slopes of the subalpine level with medium-rich soil. 30 to 50 cm high, dense grassy patches dominated by fine to medium-leaved grasses	200 (30%)	55–105	3.5 (5.1%)	high prod.
S-III	Located on medium sunny slopes in the subalpine level, very tall vegetation (over 50 cm), very dense, dominated by grasses with long, thick leaves, especially *Pazskea paniculata*	250 (55%)	30–45	0.01 (0.01%)	high prod.
S-IV	Located in flatlands and moderate slopes of the subalpine level; these herbaceous formations, dominated by nitrophilous species, develop in areas of accumulation and excess of manure	n.d.	15–55	0.17 (0.25%)	non prod.
S-V	Located on medium sunny slopes in the subalpine level, vegetation of medium height (20–30 cm), dense, dominated by *Brachypodium pinnatum*	100 (20%)	25–35	1.8 (2.7%)	medium prod.
SA-I	Located on medium and steep sunny slopes in the subalpine and alpine level, on dry and fairly deep soil. Very dense vegetation with almost 100% herbaceous cover, 30 to 50 cm high	150 (40%)	10–80	0.3 (0.4%)	medium prod.
SA-II	Located on lowlands and slopes in the subalpine or alpine level, vegetation of medium height (20–30 cm), not very dense, dominated by *Nardus stricta*	83 (37%)	20–45	12.7 (18.4%)	medium prod.
SA-III	Located on medium to steep south-facing slopes in the subalpine and alpine belt with dry soil	80 (35%)	5–40	28.2 (41.1%)	medium prod.
SA-IV	Located on very wet areas with temporary or permanent excess of water	n.d.	0–35	0.6 (0.8%)	non prod.
SA-V	Vegetation with a shrub and herb layer in the subalpine and alpine environment	n.d.	0–15	2.3 (3.4%)	non prod.
A-I	Sparse vegetation on medium to moderate slopes, windy ridges and bumps in the alpine belt	37 (35%)	5–25	13.2 (19.2%)	low prod.
A-II	Sparse vegetation in snow beds and moderate slopes in alpine, long-lasting snow environment	26 (55%)	0–30	2.7 (4.0%)	low. prod
A-III	Areas with more than 50% of the surface occupied by stones and rocks, on steep slopes, located under ridges or rock bars	n.d.	0–5	0.3 (0.5%)	non prod.

Table 2
Surface of pastures used as ground truth in this study, separated by productivity classes and by grazing area classes. Grazing area class is assigned based on the ratio of non grazeable surface to the total of the parcels. FG: fully grazeable, 95–100% of parcel area classified as pasture, HG: half grazeable (50–95%), PG: poorly grazeable (below 50%). Note that *non productive* pastures were not use for the training of Random Forest (model 3L).

Grouping criteria	Group	Surface [km2]	Surface (%)
Productivity	High productive (HP)	6.7	9.7
	Medium productive (MP)	42.7	62.2
	Low productive (LP)	16.0	23.2
	Non productive	3.4	4.9
Grazeable area	FG	15.5	22.5
	HG	21.3	31
	PG	31.9	46.5
Total		68.8 km^2	

identified areas with distinct trajectories of NDVI and NARI belonging to 1) dense forest (tree cover density 80%), 2) sparse forest (tree cover density ~30%), 3) highly productive pastures, 4) medium productive pastures, 5) low productive pastures, 6) bare soil. For each of these land cover categories we extracted average NDVI and NARI seasonal trajectories representing the templates which each pixel was compared to (supplementary material, fig. SF2). Template trajectories were modelled by means of a general additive model (GAM) with a single smooth term (as a function of time), based on thin plate regression splines (Wood et al., 2013). The DTW analysis results in an Euclidean distance map for each of the six cover categories listed above. The smaller the distance between a pixel and a template time series, the closer the vegetation dynamics of the pixel to the given template.

2.4.2. *Modelling framework*

Random forest (RF) was chosen among other machine learning algorithms because of better performance, computation speed, easier parameter tuning, and the fact that a first cross-validation is intrinsically performed with the out-of-the-bag technique (Kuhn, 2020). Moreover, random forest algorithm was proven to be successful in remote-sensing assisted mapping (e.g., Loozen et al., 2020) and in particular pasture classification in the context of climate change analysis (Dibari et al., 2020).

Three different RF were fitted to obtain three different maps: (1) the binary classification of grassland presence/absence, hereafter referred to as grassland mask (GM), (2) the grassland productivity map, i.e., the three-level classification of low, medium and high productivity (LP, MP, and HP) hereafter referred to as model 3L, and (3) the classification of the 13 pastoral categories (Section 2.2, model 13L). The `caret` package was used to fit RF models. It allows for self-tuning of the *mtry* parameter (the number of variables randomly sampled as candidates at each split) via resampling methods. We chose the repeated cross-validation method with 10-fold CV and 10 repetitions. This means that the 10-fold cross-validation is repeated 10 times, each time varying the *mtry* parameter. The parameters *mtry* of the final models chosen after self-tuning was 5 for all three models. The other three random forest parameters were deliberately kept constant for the three models, i.e., *ntree* was set to 500, *nodesize* was set to 1, as recommended for classification problems, and *maxnodes* was not set (i.e., trees can grow to the maximum possible number of terminal nodes).

Table 3 summarizes the predictors used in the models. All predictors were normalized prior to model fitting. Random forest performance was evaluated by means of the overall accuracy and the kappa (unweighted) coefficient (Cohen, 1960). A p-value from McNemar's test (McNemar, 1947) was also computed and only significant ($p<0.05$) models are discussed. When pertinent, omission and commission errors were also evaluated. For more than two classes, these errors were calculated comparing each factor level to the remaining levels (i.e., a "one versus

Table 3
Predictors used in random Forest models and their ranges (5^{th} and 95^{th} percentiles). Details on predictor calculation are provided in the text.

Predictor [m. u.]	Description	q5, q95
$NDVI_{max}$ [–]	Maximum normalized difference vegetation index, a proxy of vegetation maximum development	0.39,0.83
NARI [–]	Normalized antocyanin reflectance index, a proxy of antocyanin level in tissues	0.18,0.31
FSFD [doy]	First snow-free day, a proxy of the beginning of the growing season	84,195
GDD [°C]	Growing degree days	518,1710
AUC [–]	Area under the seasonal NDVI curve (NDVI integral, a proxy of vegetation development including phenology)	3.5,5.5
DAH [–]	Diurnalf anisotropic heating index	−0.23,0.53
$NOveg_{distance}$ [–]	DTW distance to bare soil time series	0.28,2.00
$Pasture_{distance}$ [–]	DTW distance to pasture time series	0.23,3.91

all" approach). For each of the three models, a multiple linear regression model was fitted with the same data input in order to provide a benchmark null model useful to evaluate RF model performance.

Variable importance was calculated as mean decrease in accuracy. For the 3L model, partial dependency was evaluated with the pdp R package (Greenwell, 2017).

2.4.3. Grassland mask (GM)

A subset of CDN (90 k pixels, approximately 10% of the data, randomly selected) was used for the random forest model. Data was then split: 75% was used for model training and 25% for a first assessment of validation. Model output represents a 3 level outcome (grasslands, forests and ice/water/rocks). This outcome was then converted to a binary absence/presence vector and, after prediction over the spatial extent of the GPNP, converted to a gridded grassland mask at 20 m spatial resolution (GM). Model performance was assessed trough five steps, summarized in Table 4. First, accuracy was assessed on the 25% validation subset (labelled GM-V1). Second, a confusion matrix was computed on the extent of the CDN map by comparing the predicted map GM against CDN (labelled GM-V2). This represents an extension of crossvalidation because it includes all pixels not used for training. Third, GM was compared against the Copernicus Grassland layer (labelled GM-V3). This layer is considered as a partially independent layer, being derived itself from S2-data but trough completely different processing steps compared to our approach (Copernicus, 2018b). Fourth, GM was compared against a spatial subset of the Copernicus Grassland layer (see Fig. 2), in a region of GPNP where calibration data (CDN) was not available (GM-V4). This represents a spatially independent validation. Fifth, GM accuracy was tested against the 69 km^2 mapped in PASTORALP surveys (GM-V5). Because field mapping was deliberately not exhaustive of all the grassland surfaces of the park, only omission errors could be quantified in GM-V5.

GM was used to mask out grassland productivity predictions presented in the following section.

Table 4
Random forest model characteristics and performances. Null models represent multiple linear regressions with the same predictors as RF models and were fitted for comparison only on the 25% validation exercise. Accuracy and kappa values are always obtained by computing a confusion matrix. Note that commission and omission errors are reported only on binary outcomes, i.e. for the grassland mask model. Table 5 reports omission and commission error rates for the 3L and 13L models.

Model	Validation	N calibration	N validation	Omission (%)	Commis-sion (%)	Acc./kappa (RF model)	Acc./kappa (NULL model)
Grassland mask	25% validation (**GM-V1**)	68k	22k	16	5	0.88/0.84	0.68/0.05
	GM vs CDN (**GM-V2**)	68k	927k	14	5	0.89/0.76	–
	GM vs Copernicus Grassland (all GPNP, **GM-V3**)	68k	1775k	24	15	0.76/0.54	–
	GM vs Copernicus Grassland (spatially independent, **GM-V4**)	68k	848k	26	19	0.76/0.50	–
	GM vs PASTORALP survey, **GM-V5**)	68k	155k	10	–	–	–
Productivity (**3L**)	25% validation (**3L-V1**)	25k	8k			0.90/0.84	0.72/0.50
	Full validation (FG+HG+PG) (**3L-V2**)	25k	155k			0.78/0.50	–
Pasture categories (**13L**)	25% validation (**13L-V1**)	25k	8k			0.83/0.78	–
	Full validation (FG+HG+PG) (**13L-V2**)	25k	155k			0.52/0.34	–

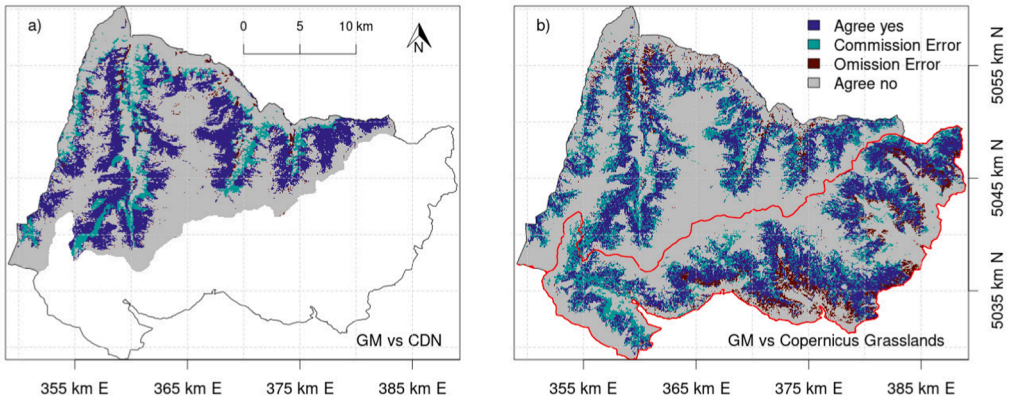

Fig. 2. Maps of the classification results for grassland detection. **a)** Comparison between grassland mask (GM) and Carta della Natura (CDN) rasterized at 20-m resolution (GM-V2, see Table 3). Dark blue pixels indicate the areas identified as grasslands in both GM and CDN. Light blue pixels are for the areas identified as grasslands in GM but not in CDN. Dark red pixels are for the areas marked as grasslands in CDN but not in GM. Grey pixels indicate the areas identified as NON grasslands in both GM and CDN. This layer was only available for a zone of the park (note the extended white areas in the South). **b)** Same as a) but against Copernicus Grassland product (GM-V4). See text for quantitative accuracy assessment. The area delimited in red corresponds to the spatial extent of validation GM-V4 in Table 3.

2.4.4. Productivity (3L) and pasture category (13L) models

Data collected in the framework of the PASTORALP project surveys was used as training data. Random forest models were trained on best-quality ground truth data, corresponding to fully grazeable areas (see Table 1 for the definition and acronyms of grazeable areas). The following validation steps are valid for both the 3L and the 13L models described above. Similar to the GM model, data was split (75% for model training and 25% for a first assessment of validation). This first type of validation is labelled 3L-V1 and 13L-V1 for the 3L and 13L models, respectively. Second, models were validated against the whole set of data from the surveys including partially grazeable surfaces (HG) and poorly grazeable surfaces (PG, see Table 2). This second validation exercise is labelled 3L-V2 and 13L-V2 for the 3L and 13L models, respectively.

The complete ground truth dataset was used to train two additional random forest models (training data constituted by FG +HG, and by FG+HG+PG), in an attempt to improve model prediction by increasing the quantity of ground truth data at the expense of its quality. These additional data sets were used to fit both 3L and 13L Models.

To examine the capacity of our models to discriminate between the various pasture types, we selected four markedly different pastoral categories (A-II, A-I , S-II, and S-I) and extracted NDVI trajectories for 500 randomly selected pixels for each category. These NDVI time series were spatially and temporally averaged resulting in an average-year trajectory for the four pasture categories.

All the statistical analyses, processing and graphics were conducted with the R Software for Statistical Computing, version 3.6.3 (R Core Team, 2020).

3. Results

3.1. Detection of grasslands

Binary classification of presence/absence of grasslands showed an excellent performance, with an accuracy of 0.88 and a kappa of 0.84 in validation (GM-V1, Table 4). Correspondent NULL model (i.e. a multiple regression with the same predictors) showed much lower accuracy (0.68) and a decline in kappa (0.05). The random forest model was then used to predict a binary presence/absence classification map at the scale of the Park (grassland mask, GM). GM was compared against CDN (GM-V2) and the Copernicus Grassland layer (GM-V3, Fig. 2). Classification scores remained high when computed against the CDN map (accuracy 0.89, kappa 0.76), with a sensitivity of 86% (omission error 14%) and a specificity of 95% (commission error 5%). The classification score assessment against Copernicus Grassland (a partially independent data set, because it is also derived from S-2 data) showed fairly good accuracy (0.76) and a lower kappa (0.54). The sensitivity and specificity (and correspondent omission and commission error) were 76% (24%) and 85% (15%), respectively. GM was furthermore validated against a spatial subset of Copernicus Grassland (area delimited in red in Fig. 2b). Accuracy and kappa were 0.76 and 0.50, respectively. GM accuracy (omission error only) was tested also against the 69 km^2 mapped in the PASTORALP survey, and omission error was found to be 10%.

Variable importance analysis shows that NDVI was the most important predictor, followed by $DTW_{distance}$ to low productive pastures, $DTW_{distance}$ to bare ground and growing degree days (supplementary material, fig. SF3). Remaining predictors showed only very limited explanatory power.

3.2. Prediction of productivity

The model for the discrimination of 3 productivity levels (model 3L) showed a high accuracy (0.90) and kappa (0.84) in 25% validation (3L-V1, Table 4). Correspondent NULL model (i.e. a multiple regression with the same predictors) showed much lower accuracy (0.72) and kappa (0.50). Omission and commission errors associated to each of the three productivity levels are reported in Table 5. 3L model was also validated against the whole surveyed surface (i.e. including partially grazeable areas, FG+HG+PG). Accuracy was 0.78 and kappa 0.50 (3L-V2, Table 4).

Variable importance analysis revealed that GDD was the most important variable, followed by FSFD, NDVI, AUC and DAH, which however showed about one third of the GDD importance (supplementary material, fig. SF4).

The distribution of S2-derived LAI and NDVI values extracted from pixels classified as high, medium and low in the 3L classification showed distinct ranges, with increasing LAI and NDVI corresponding to increasing levels of predicted productivity (Fig. 3).

3.2.1. Prediction of pasture categories

The prediction of the 13 pastoral categories (model 13L, Table 5, Fig. 4) showed a slightly lower performance compared to the model 3L. Accuracy was found to be 0.83 and kappa 0.78 for the 25% validation (13L-V1). Commission and omission errors were calculated for the 10 most widespread categories (i.e., those predicted to cover more than 2 hectares) and are reported in Table 5. In general, less represented pastoral categories tend to show omission errors higher than 20–30%, while the most widespread categories show omission errors around or below 15% (Dibari et al., 2020). Commission errors are consistently much lower (6% or less). Similar to model 3L, 13L model was validated against the whole surveyed surfaces. Accuracy and kappa were found to be 0.52 and 0.34, respectively.

Variable importance analysis for the model 13L showed that, similar to the model 3L, GDD was the most important one. DAH and FSFD

Table 5
Classification scores for grassland productivity models tested in this study. LP: low productive, MP: medium productive, HP: high productive. We report error rates of the 10 pastoral categories (out of 13 analysed) predicted to cover a surface larger than 2 hectares. For category names and full description, please refer to Table 1. Omission and commission errors refer to validations labelled 3L-V1 and 13L-V1 for model 3L and 13L, respectively.

Model	Productivity/Pasture category	Surface predicted (km^2)	Omission error (%)	Commission error (%)	Accuracy	kappa
model 3L	LP	66	9.7	3.0	**0.90**	**0.84**
	MP	197	6.9	12.3		
	HP	32	16.7	2.3		
model 13L	SA-III	181	10.6	6.1	**0.83**	**0.78**
	SA-II	27	17.6	5.9		
	A-I	52	12.7	3.8		
	S-I	12	7.2	2.1		
	S-II	5.4	33.5	1.7		
	A-II	5.2	35.1	1.5		
	S-V	3.2	25.2	0.6		
	SA-IV	0.45	73.5	0.1		
	S-IV	0.15	65.1	0.0		
	SA-V	7.68	35.0	0.1		

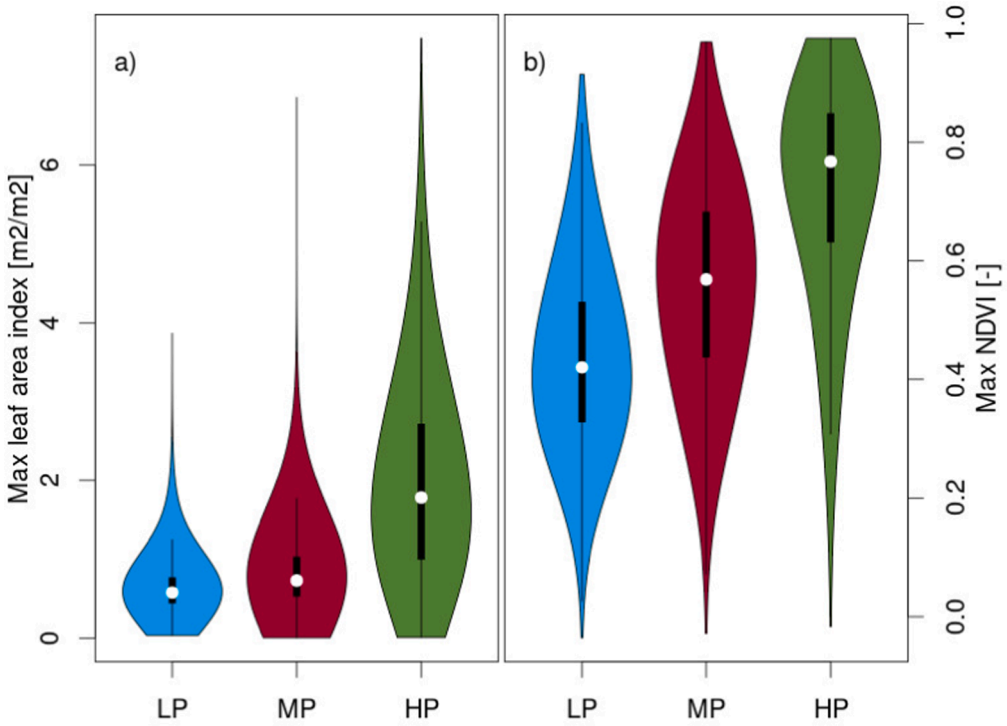

Fig. 3. Violin plot (a combination of density and box plot) showing values of **a)** Leaf Area Index (LAI, max composite for the period 2017–2019, Sentinel-2 biophysical processor) and **b)** NDVI (max composite for the period 2017–2019) extracted from all pixels classified as high, medium and low productive pastures.

followed with half the importance of GDD (supplementary material, fig. SF5).

Spatio-temporal average NDVI trajectories for the four selected pasture categories (Fig. 5) showed different NDVI peak absolute values, and different phenology, particularly for the beginning of the growing period, which showed a difference larger than 2 months between lower-elevation productive grasslands (S-I) and high-elevation pastures of the nival belt (A-II).

Performances of the additional random forest models trained on lower quality ground truth data, i.e., including also parcels with partially grazeable surfaces (FG+HG, and FG+HG+PG) are reported in Table 6. Scores were higher for model fit with best quality parcels as ground truth (FG) even though they represent only 20% of the ground truth data, and decrease when HG and PG areas are included in the training set.

4. Discussion

In this study, we used random forest models to predict the distribution and the productivity of grassland surfaces in a topographically complex Alpine protected area (Gran Paradiso National Park, 710 km^2) in north-western Italy. We built on a massive terrain vegetation survey as ground truth, and on remote-sensing-derived, climatic and topographic layers as predictors. We had three objectives: 1) the detection of herbaceous surfaces at 20 m spatial resolution, 2) the classification of pastoral surfaces in productivity classes and 3) the discrimination of thirteen pastoral categories.

4.1. Detection of grasslands

We predicted a total grassland area of 300 km^2, corresponding to ~ 42% of the GPNP surface.

The distribution of grassland surfaces (grassland mask, GM) was modelled with an accuracy ranging between 0.76 and 0.88, depending on the product used as ground truth (i.e., CDN or Copernicus Grassland). Pazúr et al. (2021) classified grassland distribution using random forest classifiers across the whole Switzerland achieving accuracies ranging between 0.85 and 0.93, depending on the layers used for comparison. Similarly, Guo et al. (2020) reported accuracies of 0.85–0.96 in mountain grassland detection in China, using deep learning methods. These results, obtained in similar environments, and with comparable approaches, are in line with our findings. Some studies coupled multi-source optical remote sensing with other data sources such as SAR, followed by data reduction techniques (Badreldin et al., 2021) achieving even higher classification performances (0.96–0.99). However, the use of SAR data in mountain areas is strongly limited by the effect of complex topography on backscattering (Imperatore, 2021).

It must be noted that the definition of ground truth is not trivial, because the two comparative maps against which we tested our product (GM-V2, GM-V3, GM-V4) cannot be considered error-free and the question remains, whether disagreement between maps can be attributed to an error of GM or in the so-called ground truth. A quantitative accuracy assessment for CDN is currently lacking, preventing any further evaluation. The accuracy assessment of the Copernicus Grassland Product reported a 0.92 overall accuracy, 25% omission error, and 24% commission error in the Alpine region (Copernicus, 2018a). A direct comparison of our classification scores with Copernicus accuracy assessment is clearly not possible, but the fact that scores in our study display the same range, if not smaller, corroborates the robustness of our approach. A large portion of omission errors is distributed in the south-eastern part of the park (Fig. 2b), where ground truth data from CDN was missing, corresponding to the white areas of Fig. 2a. We regarded this area (delimited by the red border in Fig. 2b), as a spatially independent subset to evaluate model performance in an area excluded from the training, and found a very limited decrease of model performance (Table 5). This indicates the robustness of our model even in spatially independent areas. However, models such the ones developed in this work must be used with caution in pure prediction, paying particular attention that the range of predictors in calibration areas (cfr. Table 3) be consistent with those in areas to be predicted.

Commission errors against Copernicus Grassland product are about four times higher than omission errors, occur more often at high

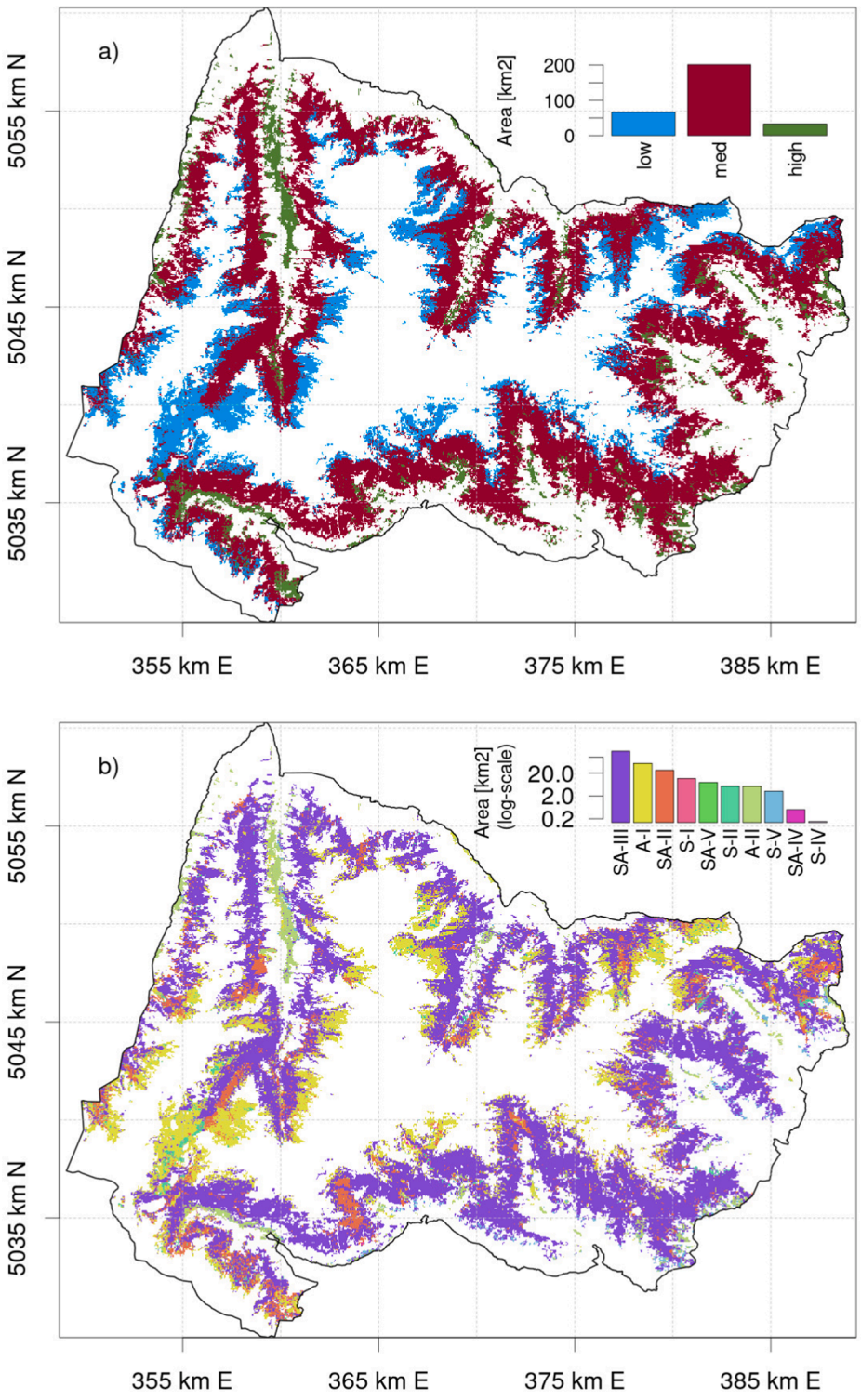

Fig. 4. Prediction maps for GPNP. **a)** Three level productivity map, **b)** Pastoral categories map. Inset: histograms of areas for categories displayed in the maps. For category names and full description, please refer to Table 1 and supplementary ST2.

elevation, across a wider range of NDVI values, and mainly in locations with no tree cover (Fig. 6). By comparing with the original land cover map (CDN, photo-interpreted), we found that only ~25% of commission error pixels are misclassified as forest (15%) or shrub (10%) pixels, whereas the remaining 75% are grass-covered surfaces. Even tough this comparison is conducted against a relatively old layer (CDN dates back to 2006), and therefore the percentages must be considered as indicative, these areas deserve attention. They were not classified as grasslands in 2018 (the date of Copernicus product), display however a NDVI peak higher than 0.25 and cannot be considered as bare soil. These findings suggest that according to our classification, high elevation areas with sparse herbaceous vegetation are present, and confirm conclusions of a recent alpine-wide study (Choler et al., 2021). These areas, on the edge between recently colonized bare ground/debris and true grasslands but displaying a highly dynamic evolution towards the second group, potentially represent newly available grass resources not currently

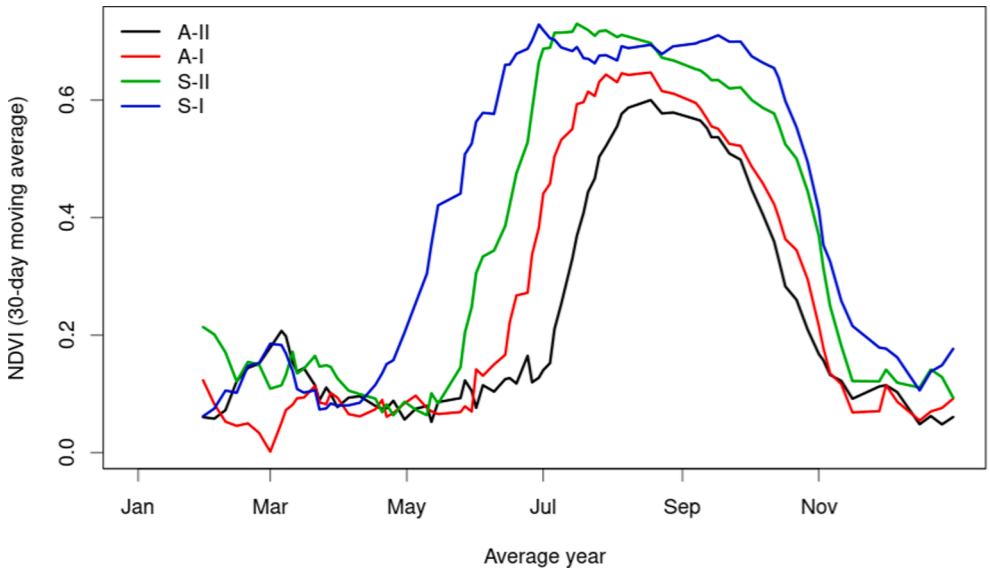

Fig. 5. Average-year trajectories of NDVI for four different pastoral categories. NDVI was extracted from multitemporal Sentinel-2 images, aggregated across 500 randomly-selected pixels and over time (period 2017–2019). For category names and full description, please refer to Table 1.

Table 6
Classification scores for pasture productivity models trained with data sets with different levels of net grazeable area. FG: fully grazeable, HG: half-grazeable, PG: poorly grazeable, 3L: three levels productivity model, 13L: productivity model with the 13 pastoral categories.

Metric	FG model 3L	FG+HG model 3L	FG+HG+PG model 3L	FG model 13L	FG+HG model 13L	FG+HG+PG model 13L
Accuracy	0.90	0.88	0.87	0.83	0.78	0.76
kappa	0.84	0.77	0.72	0.78	0.71	0.66

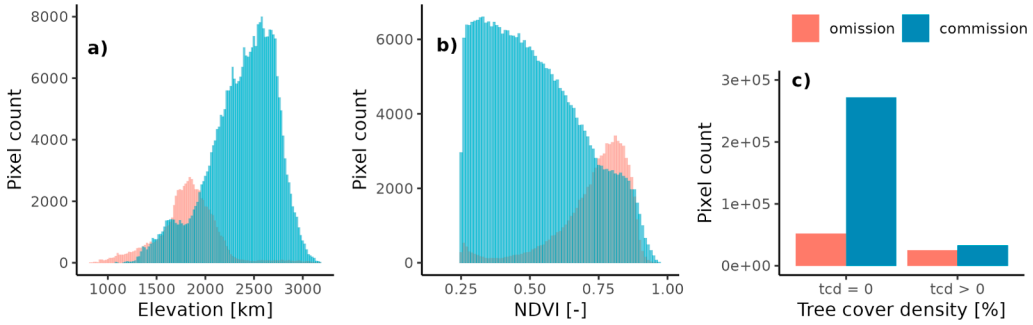

Fig. 6. Distribution of selected variables in pixels displaying omission and commission errors. **a)** Histograms of elevation values of pixels displaying omission and commission errors, **b)** same as a) but for NDVI, **c)** Count of pixels displaying omission and commission for two classes of tree cover density.

exploited for domestic pasture, but likely grazed by wild animals. Hence, the detailed quantification of these surfaces is a key information for the management, especially in protected areas such as GPNP.

4.2. *Prediction of productivity and pasture categories*

The distribution of pasture categories was predicted with an accuracy ranging from 0.83, for the 13-level classification (pasture categories, 13L), up to 0.90 for the three levels classification (productivity, 3L). In contrast to the determination of grassland surfaces, an independent product to quantitatively assess classification performance is not available. However, historical above ground biomass estimations (Table 1) allowed us to directly link pastoral categories with productivity. Accordingly, we used a maximum composite Leaf Area Index at 20-m spatial resolution (a standard product derived from Sentinel-2 biophysical processor) as an estimate of productivity and qualitatively evaluated the distribution of LAI and NDVI values from all pixels classified as high, medium and low productive (Fig. 3). Distinct ranges of both LAI and NDVI across the three productivity levels support the robustness of our classification approach, that can be used for e.g. carrying capacity estimation on large areas (Yu et al., 2010).

In order to assess the validity of the pastoral classification, we evaluated NDVI seasonal trajectories extracted from pure pasture polygons belonging to a subgroup of pastoral categories. In order to showcase the different NDVI trajectories across the range of different pasture categories, we chose S-I and S-II pastures as representative of the high productive class, and A-I and A-II as representative of the low productive class. NDVI trajectories show marked differences among pastoral categories in terms of phenology (beginning of the growing season), maximum NDVI values and shape of the seasonal curve, further confirming the validity of our classification approach.

4.3. Biophysical significance of RF predictors

Machine learning algorithms such as random forests are usually considered as black boxes, making it difficult to find causal relationships between predictors and a given outcome. However, the partial dependence plots of the most important predictors (e.g., GDD, FSFD, NDVImax, fig. SF6) suggest the presence of relevant thresholds in predictors. For example low productive grasslands were prevalent with GDD $<$ 800°C and their occurrence probability dropped when GDD exceeded this threshold. Similarly, at approximately 1700°C GDD, the probability of occurrence of high productive grasslands became prevalent as compared to mid productive ones. AUC displayed a clear break in probability around the value of 4, above which the occurrence of mid productive pastures becomes more likely compared to low productive ones, whereas high productive pasture probability occurrence is rather insensitive to AUC changes. Similar thresholds, although less clear compared to GDD or AUC, can be hypothesised for FSFD and NDVImax. Further studies will help to clarify whether these thresholds are study-specific or may be considered valid at larger spatial scales.

4.4. Quality vs spatial coverage of ground truth data

In this study, field data (PASTORALP survey) was collected for management purposes, but also with the objective of building a sound ground truth data set for remote sensing-based classification. Accordingly, special attention was devoted to the quantification of non-grazeable surfaces within pastoral parcels, which include single trees, shrubs, buildings, roads, and severely impact the quality of signals detected from space. This led to an invaluable data set that allowed us to quantify the sensitivity of predictive modelling to data quality and quantity. A total area of 69 km^2 of pastures was mapped, but only ~20%, 15 km^2 of fully grazeable surfaces were used as the training set for random forest models (3L, 13L, Table 2). Including the remaining ~80% of pastoral surfaces in the training set did not add predictive power nor increased model performance. We conclude, that the quality of ground truth data is much more important than its spatial coverage for the classification of pastoral categories in Alpine terrains. This information may be useful to design ground truth data collection for similar classification purposes, especially in complex landscapes such as the alpine and subalpine belts. By concentrating field effort on pure pastoral surfaces, a high level of accuracy can be achieved with cheaper, shorter and tailored sampling campaigns.

Classification performances decreased when models were validated against the whole PASTORALP surveys, i.e., including partially and poorly grazeable surfaces, especially for 13L model (Table 4). This is likely because the classification at 20 m spatial resolution is able to retrieve sub - parcel information that the ground truth survey levelled out by assigning the class/category at the parcel level, thus neglecting small-scale heterogeneity that the pixel-based classification retains.

5. Conclusions

A great, currently unresolved challenge for the management of alpine pastoral resources is represented by their accurate quantification. In this work, we modelled grassland presence/absence, pastoral productivity and categories based on a massive field campaign and satellite-derived predictors in the Gran Paradiso National Park, a 710 km^2 protected area in the north-western Alps. We demonstrated that a high accuracy can be achieved with a tailored field campaign that focuses sampling effort on pure pastoral surfaces. Resulting data can be combined with the state-of-the-art, publicly available satellite products to train random forest classification models, in turn used to predict grassland distribution and productivity with high accuracy and spatial detail even in complex mountainous landscapes. This approach can be transferred in space and time, thus representing a potentially strong contribution to the management of Alpine grasslands, and to the construction of adaptation strategies to climate and land use change.

Declaration of Competing Interest

The authors declare that they have no known competing financial interests or personal relationships that could have appeared to influence the work reported in this paper.

Acknowledgments

This research was supported by the LIFE PASTORALP project (LIFE16 CCA/IT/000060), co-funded by the European Union's LIFE Programme, Climate change adaptation action sub-programme, by the ANR TOP project, grant ANR-20-CE32-0002 of the French Agence Nationale de la Recherche. LECA is part of OSUG@2020 labex (reference ANR10 LABX56).

The authors sincerely thank Valentina Andreo, Roberta Benetti, Giampaolo Bruno, Mauro Coppa, Maurizio Odasso and Camilla Scalabrini for the tireless and diligent work in the field surveys.

Appendix A. Supplementary material

Supplementary data associated with this article can be found, in the online version, at https://doi.org/10.1016/j.jag.2022.102718.

References

Abdi, A.M., 2020. Land cover and land use classification performance of machine learning algorithms in a boreal landscape using Sentinel-2 data. GISci. Remote Sens. 57 (1), 1–20.

Argenti, G., Bassignana, M., Bellocchi, G., Dibari, C., Filippa, G., Poggio, L., Staglianò, N., Bindi, M., 2018. LIFE PASTORALP: a project for alpine pasture vulnerability assessment. In: L'agronomia nelle nuove agriculturae, Società Italiana di Agronomia, pp. 174–175.

Badreldin, N., Prieto, B., Fisher, R., 2021. Mapping grasslands in mixed grassland ecoregion of saskatchewan using big remote sensing data and machine learning. Remote Sens. 13, 4972.

Bassignana, M., Piccot, A., Cremonese, E., Filippa, G., Galvagno, M., Choler, P., Bayle, A., Poggio, L., 2021. Deliverable C2 Pastures typologies survey and mapping. URL: https://www.pastoralp.eu/wp-content/uploads/2021/05/Deliverable_C2_final_21.05.21.pdf.

Bayle, A., Carlson, B.Z., Thierion, V., Isenmann, M., Choler, P., 2019. Improved Mapping of Mountain Shrublands Using the Sentinel-2 Red-Edge Band. Remote Sens. 11 (23).

Böhner, J., Antonic, O., 2009. Chapter 8 Land-Surface Parameters Specific to Topo-Climatology. In: Hengl, T., Reuter, H.I. (Eds.), Geomorphometry. Developments in Soil Science, vol. 33. Elsevier, pp. 195–226.

Bornard, A., Bassignana, M., Bernard-Brunet, C., Labonne, S., Cozic, P., 2006. Les végétations d'alpage de la Vanoise. Description agro-écologique et gestion pastorale. Quae Editions, Versailles.

Buchhorn, M., Smets, B., Bertels, L., Lesiv, M., Tsendbazar, N.-E., Herold, M., Fritz, S., october 2019. Copernicus Global Land Service: Land Cover 100m: collection 2: epoch 2015: Globe.

Canedoli, C., Ferrè, C., Abu El Khair, D., Comolli, R., Liga, C., Mazzucchelli, F., Proietto, A., Rota, N., Colombo, G., Bassano, B., Viterbi, R., Padoa-Schioppa, E., 2020. Evaluation of ecosystem services in a protected mountain area: Soil organic carbon stock and biodiversity in alpine forests and grasslands. Ecosyst. Serv. 44, 101135.

Cavallero, A., Aceto, P., Gorlier, A., Lombardi, G., Lonati, M., Martinasso, B., Tagliatori, C., 2007. I tipi pastorali delle Alpi piemontesi. Alberto Perdisa Editore.

Chang, J., Ciais, P., Gasser, T., Smith, P., Herrero, M., Havlík, P., Obersteiner, M., Guenet, B., Goll, D., Li, W., Naipal, V., Peng, S., Qiu, C., Tian, H., Viovy, N., Yue, C., Zhu, D., 2021. Climate warming from managed grasslands cancels the cooling effect of carbon sinks in sparsely grazed and natural grasslands. Nature Communications 12.

Choler, P., 2018. Winter soil temperature dependence of alpine plant distribution: Implications for anticipating vegetation changes under a warming climate. Perspect. Plant Ecol. Evol. Syst. 30, 6–15 (special issue on Alpine and arctic plant communities: a worldwide perspective). URL: https://www.sciencedirect.com/science/article/pii/S1433831917300288.

Choler, P., Bayle, A., Carlson, B.Z., Randin, C., Filippa, G., Cremonese, E., 2021. The tempo of greening in the European Alps: Spatial variations on a common theme. Glob. Change Biol. 27 (21), 5614–5628.

Cohen, J., 1960. A coefficient of agreement for nominal scales. Educ. Psychol. Measur. 20 (1), 37–46.

Conant, R.T., Food, of the United Nations., A.O., 2010. Challenges and opportunities for carbon sequestration in grassland systems: a technical report on grassland management and climate mitigation/ Prepared for the Plant Production and Protection Division, Food and Agriculture Organization of the United Nations (FAO),

compiled by Richard T. Conant. Food and Agriculture Organization of the United Nations Rome.
Copernicus, 2018a. CLMS Land Product Validation, High Resolution Layer Grassland 2018. URL: https://land.copernicus.eu/user-corner/technical-library/clms_hrl_gra_validation_report_sc04_v1_5.pdf.
Copernicus, 2018b. European Grassland distribution, 10 m spatial resolution. URL: https://land.copernicus.eu/pan-european/high-resolution-layers/grassland/status-maps/grassland-2018.
Copernicus, 2018c. Tree Cover Density, 100 m spatial resolution. URL: https://land.copernicus.eu/pan-european/high-resolution-layers/forests/tree-cover-density/status-maps/2018.
Crabbe, R.A., Lamb, D., Edwards, C., 2020. Discrimination of species composition types of a grazed pasture landscape using Sentinel-1 and Sentinel-2 data. Int. J. Appl. Earth Obs. Geoinf. 84, 101978.
Dibari, C., Bindi, M., Moriondo, M., Staglianó, N., Targetti, S., Argenti, G., 2016. Spatial data integration for the environmental characterization of pasture macrotypes in the Italian Alps. Grass Forage Sci. 71.
Dibari, C., Costafreda-Aumedes, S., Argenti, G., Bindi, M., Carotenuto, F., Moriondo, M., Padovan, G., Pardini, A., Staglianó, N., Vagnoli, C., Brilli, L., 2020. Expected changes to alpine pastures in extent and composition under future climate conditions. Agronomy 10 (7).
Dibari, C., Pulina, A., Argenti, G., Aglietti, C., Bindi, M., Moriondo, M., Mula, L., Pasqui, M., Seddaiu, G., Roggero, P.P., 2021. Climate change impacts on the Alpine, Continental and Mediterranean grassland systems of Italy: A review. Italian J. Agron. 16.
Farr, T.G., Rosen, P.A., Caro, E., Crippen, R., Duren, R., Hensley, S., Kobrick, M., Paller, M., Rodriguez, E., Roth, L., Seal, D., Shaffer, S., Shimada, J., Umland, J., Werner, M., Oskin, M., Burbank, D., Alsdorf, D., 2007. The Shuttle Radar Topography Mission. Rev. Geophys. 45 (2).
Filippa, G., Cremonese, E., Galvagno, M., Isabellon, M., Bayle, A., Choler, P., Carlson, B. Z., Gabellani, S., Morra di Cella, U., Migliavacca, M., 2019. Climatic Drivers of Greening Trends in the Alps. Remote Sens. 11 (21).
Garbarino, M., Morresi, D., Urbinati, C., Malandra, F., Motta, R., Sibona, E., Vitali, A., Weisberg, P., 2020. Contrasting land use legacy effects on forest landscape dynamics in the Italian Alps and the Apennines. Landscape Ecol. 12, 35.
Gascoin, S., Grizonnet, M., Bouchet, M., Salgues, G., Hagolle, O., 2019. Theia Snow collection: high-resolution operational snow cover maps from Sentinel-2 and Landsat-8 data. Earth Syst. Sci. Data 11 (2), 493–514.
Giorgino, T., 2009. Computing and Visualizing Dynamic Time Warping Alignments in R: The dtw Package. J. Stat. Softw. Articles 31 (7), 1–24.
Greenwell, B.M., 2017. pdp: An r package for constructing partial dependence plots. R J. 9 (1), 421–436. URL https://journal.r-project.org/archive/2017/RJ-2017-016/index.html.
Griffiths, P., Nendel, C., Pickert, J., Hostert, P., 2020. Towards national-scale characterization of grassland use intensity from integrated sentinel-2 and landsat time series. Remote Sens. Environ. 238, 111124 time Series Analysis with High Spatial Resolution Imagery. URL: https://www.sciencedirect.com/science/article/pii/S0034425719301087.
Guo, Z., Liu, H., Zheng, Z., Chen, X., Liang, Y., 2020. Accurate extraction of mountain grassland from remote sensing image using a capsule network. In: IEEE Geosci. Remote Sens. Lett., pp. 1–5.
Herzog, F., Seidl, I., 2018. Swiss alpine summer farming: current status and future development under climate change. Rangeland J. 40.
Hinojosa, L., Tasser, E., Rüdisser, J., Leitinger, G., Schermer, M., Lambin, E., Tappeiner, U., 2019. Geographical heterogeneity in mountain grasslands dynamics in the Austrian-Italian Tyrol region. Appl. Geogr. 106, 50–59.
Imperatore, P., 2021. Sar imaging distortions induced by topography: A compact analytical formulation for radiometric calibration. Remote Sens. 13, 3318.
Jouglet, J., 1999. Les végétations des alpages des alpes françaises du sud; guide technique pour la reconnaissance et la gestion des milieux pâturés d'altitude.
Kolecka, N., Ginzler, C., Pazur, R., Price, B., Verburg, P., 2018. Regional Scale Mapping of Grassland Mowing Frequency with Sentinel-2 Time Series. Remote Sens. 10, 1221.
Körner, C., 2004. Mountain Biodiversity, its Causes and Function. AMBIO: J. Hum. Environ. 33 (sp13), 11–17.
Kuhn, M., 2020. caret: Classification and Regression Training. R package version 6.0-86. URL: https://CRAN.R-project.org/package=caret.
Loozen, Y., Rebel, K., De Jong, S., Lu, M., Ollinger, S., Wassen, M., Karssenberg, D., 2020. Mapping canopy nitrogen in European forests using remote sensing and environmental variables with the random forests method. Remote Sens. Environ. 247, 111933.
Magiera, A., Feilhauer, H., Waldhardt, R., Wiesmair, M., Otte, A., 2017. Modelling biomass of mountainous grasslands by including a species composition map. Ecol. Ind. 78, 8–18.
Maus, V., Câmara, G., Appel, M., Pebesma, E., 2019. dtwSat: Time-Weighted Dynamic Time Warping for Satellite Image Time Series Analysis in R. J. Statist. Softw. Articles 88 (5), 1–31.
McNemar, Q., 1947. Note on the sampling error of the difference between correlated proportions or percentages. Psychometrika 12 (2), 153–157.
Monteiro, A.T., Carvalho-Santos, C., Lucas, R., Rocha, J., Costa, N., Giamberini, M., Costa, E.M. d., Fava, F., 2021. Progress in grassland cover conservation in southern european mountains by 2020: A transboundary assessment in the iberian peninsula with satellite observations (2002–2019). Remote Sens. 13(15).
Orlandi, S., Probo, M., Sitzia, T., Trentanovi, G., Garbarino, M., Lombardi, G., Lonati, M., 2016. Environmental and land use determinants of grassland patch diversity in the western and eastern Alps under agro-pastoral abandonment. Biodivers. Conserv. 25, 275–293.
Pazúr, R., Huber, N., Weber, D., Ginzler, C., Price, B., 2021. A national extent map of cropland and grassland for switzerland based on sentinel-2 data. Earth Syst. Sci. Data Discuss. 2021, 1–14. URL https://essd.copernicus.org/preprints/essd-2021-60/.
Phiri, D., Simwanda, M., Salekin, S., Nyirenda, V.R., Murayama, Y., Ranagalage, M., 2020. Sentinel-2 Data for Land Cover/Use Mapping: A Review. Remote Sens. 12 (14).
Pittarello, M., Probo, M., Perotti, E., Lonati, M., Lombardi, G., Ravetto Enri, S., 2019. Grazing management plans improve pasture selection by cattle and forage quality in sub-alpine and alpine grasslands. J. Mount. Sci. 16, 2126–2135.
Ponzetta, M., Cervasio, F., Crocetti, C., Messeri, A., Argenti, G., 2010. Habitat improvements with wildlife purposes in a grazed area on the Appennine Mountains. Italian J. Agron. 10, 5.
Pornaro, C., Basso, E., Macolino, S., 2019. Pasture botanical composition and forage quality at farm scale: A case study. Italian J. Agron. 14, 214–221.
Punalekar, S., Planque, C., Lucas, R., Evans, D., Correia, V., Owers, C., Poslajko, P., Bunting, P., Chognard, S., 2021. National scale mapping of larch plantations for Wales using the Sentinel-2 data archive. For. Ecol. Manage. 501.
R Core Team, 2020. R: A Language and Environment for Statistical Computing. R Foundation for Statistical Computing, Vienna, Austria. URL: https://www.R-project.org/.
Ramankutty, N., Evan, A.T., Monfreda, C., Foley, J.A., 2008. Farming the planet: 1. geographic distribution of global agricultural lands in the year 2000. Global Biogeochem. Cycles 22 (1).
Reinermann, S., Asam, S., Kuenzer, C., 2020. Remote Sensing of Grassland Production and Management - A Review. Remote Sens. 12 (12).
Schwieder, M., Wesemeyer, M., Frantz, D., Pfoch, K., Erasmi, S., Pickert, J., Nendel, C., Hostert, P., 2022. Mapping grassland mowing events across germany based on combined sentinel-2 and landsat 8 time series. Remote Sens. Environ. 269, 112795. URL https://www.sciencedirect.com/science/article/pii/S0034425721005150.
Silvestro, F., Gabellani, S., Delogu, F., Rudari, R., Boni, G., 2013. Exploiting remote sensing land surface temperature in distributed hydrological modelling: The example of the Continuum model. Hydrol. Earth Syst. Sci. 17, 39–62.
Silvestro, F., Gabellani, S., Rudari, R., Delogu, F., Laiolo, P., Boni, G., 2015. Uncertainty reduction and parameter estimation of a distributed hydrological model with ground and remote-sensing data. Hydrol. Earth Syst. Sci. 19, 1727–1751.
Urbina, I., Grau, O., Sardans, J., Ninot, J., Penuelas, J., 2020. Encroachment of shrubs into subalpine grasslands in the Pyrenees changes the plant-soil stoichiometry spectrum. Plant Soil 1–17.
Weiss, M., Baret, F., 2016. S2toolbox level 2 products: Lai, fapar, fcover v1.1. URL: https://step.esa.int/docs/extra/ATBD_S2ToolBox_L2B_V1.1.pdf.
Wood, S., Scheipl, F., Faraway, J., 2013. Straightforward intermediate rank tensor product smoothing in mixed models. Statist. Comput. 23.
Xie, Q., Dash, J., Huete, A., Jiang, A., Yin, G., Ding, Y., Peng, D., Hall, C.C., Brown, L., Shi, Y., Ye, H., Dong, Y., Huang, W., 2019. Retrieval of crop biophysical parameters from Sentinel-2 remote sensing imagery. Int. J. Appl. Earth Obs. Geoinf. 80, 187–195.
Yu, L., Li, Z., Wei, L., Hua-Kun, Z., L, Z., Liu, L., Zhou, W., 2010. Using Remote Sensing and GIS Technologies to Estimate Grass Yield and Livestock Carrying Capacity of Alpine Grasslands in Golog Prefecture, China. Pedosphere 20, 342–351.